Tone Dependent Color Error Diffusion

Project Report

Multidimensional DSP, Spring 2003

Vishal Monga

Abstract

Conventional grayscale error diffusion halftoning produces worms and other objectionable artifacts. Tone Dependent error diffusion for grayscale halftoning (Li and Allebach) helps reduce these artifacts by controlling diffusion of quantization errors based on the input graylevel value. Allebach *et al.* design error filters weights and thresholds for each (input) graylevel optimized based on a human visual system (HVS) model. In this report we extend tone dependent error diffusion to color. A visually optimum deisgn approach for tone dependent error filters (for each color plane) is presented. The resulting halftones are seen to overcome most of the traditional error diffusion artifacts.

I. Introduction

Digital Halftoning is the process of transforming a continuous tone image (grayscale or color) to an image with reduced number of levels so that it can be displayed (or printed) on devices with limited reproduction palettes. Common examples are converting an eight-bit per pixel grayscale image to a binary image, and a 24-bit color image (with eight bits per pixel per color) to a three-bit color image.

In grayscale halftoning by error diffusion, each grayscale pixel is thresholded to white or black, and the quantization error is fed back, filtered, and added to the neighboring grayscale pixels [1]. Although an error filter is typically lowpass, the feedback arrangement causes the quantization error to be highpass filtered, i.e. pushed into high frequencies where the human eye is least sensitive. The original error diffusion halftoning algorithm by Floyd and Steinberg is known to produce halftone images with smooth texture in slowly varying regions and sharp rendering of detail [1]. However, it also suffers from worms and other objectionable artifacts. Many error diffusion variations and enhancements have been developed to improve halftone quality, which includes using variable thresholds [2], [3], [4], variable weights [5] and different scan paths [6].

Recently, tone dependent error diffusion methods have been developed for grayscale error diffusion [7], [8]. These methods include using error filters with different values for different graylevels in the input image. The quantizer threshold is also modulated based on the input graylevel [7]. In this project, we formulate the

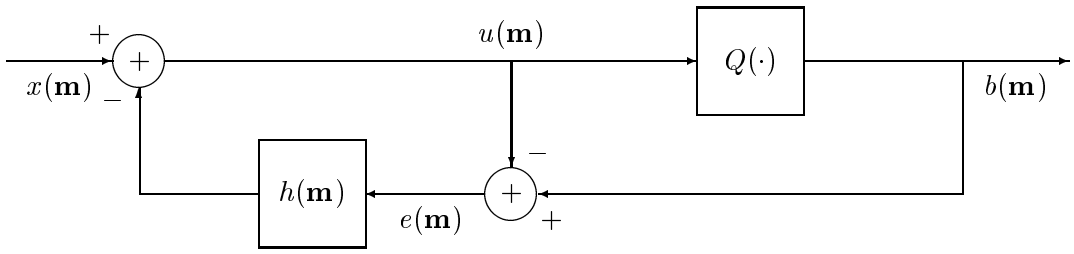

Fig. 1. System block diagram for grayscale error diffusion halftoning where $\mathbf{m}$ represents a two-dimensional spatial index (m_1, m_2) and $h(\mathbf{m})$ is a fixed 2-D nonseparable FIR error filter

design of tone dependent color error diffusion halftoning systems. The design procedure trains error filters for each color plane to minimize the perceived error between a constant valued continuous tone color image and its corresponding halftone pattern. A color human visual system (HVS) model takes into account the correlation amongst color planes. The color HVS model that we employ, is based on a transformation to the Linearized CIELab color space [9] and exploits the spatial frequency sensitivity variation of the luminance and chrominance channels in the Linearized CIELab representation. The efficacy of Linearized CIELab in computing color reproduction errors in halftoning is shown in [10]. The resulting halftones overcome many of the artifacts associated with traditional error diffusion viz. worms/directional artifacts and false textures. The color HVS model helps minimize the visibility of the halftone pattern.

Section II briefly reviews ideas in grayscale tone dependent error diffusion halftoning. The color HVS model used in error filter design is described in Section III. Section IV formulates the design problem for tone dependent color error diffusion. Section V compares color halftones generated by the proposed method with traditional color error diffused halftones. Section VI summarizes the contributions of the report and concludes with open research problems.

II. Grayscale Tone Dependent Error Diffusion

Grayscale error diffusion halftoning effectively shapes the quantization error into high frequencies, where the human eye is less sensitive. The system block diagram shown in Fig. 1, is also known as a noise-shaping feedback coder. The design of the error filter $h(\mathbf{m})$ holds the key to the quality of the generated halftone.

Tone dependent error diffusion methods involve using error diffusion filters with different sizes and values for different graylevels [7], [8]. Optimal error weighting matrix design for selected graylevels based on "blue-noise" spectra was introduced in [11]. The tone dependent error diffusion (TDED) algorithm in [7] searches for error filter weights and thresholds to minimize a visual cost function for each input graylevel.

The threshold matrix used by Li and Allebach [7] is based on a binary DBS pattern for a constant input of mid-gray. For the error filter design, the authors chose the magnitude of the DFT of the DBS pattern as an objective spectrum for the halftone pattern for input graylevel values in the midtones (21-234). For the highlight and shadow regions (graylevel values in 0-20 and 235-255) the objective spectrum is the DFT of the graylevel patch. For color error diffusion, independent design for each color plane would ignore the correlation amongst color planes . The criterion for the error filter design must hence be based on a color HVS model. The perceptual model used in our design is explained next.

III. Perceptual Model

This section describes the model for calculating the perceived halftone image. First, we define the Linearized CIELab color space in which the minimization of the squared perceived error will be performed. The frequency response of channel-separable human visual model is then described.

A. Linearized Uniform Color Space

The linearized CIELab color space is obtained by linearizing the CIELab space about the D65 white point [9] in the following manner:

$$Y_y = 116\,\frac{Y}{Y_n} - 16 \tag{1}$$

$$C_x = 500\left[\frac{X}{X_n} - \frac{Y}{Y_n}\right] \tag{2}$$

$$C_z = 200\left[\frac{Y}{Y_n} - \frac{Z}{Z_n}\right] \tag{3}$$

The Y_y component is proportional to the luminance and the C_x and C_z components are similar to the R-G and B-Y opponent color chrominance components on which Mullen's data [12] is based. The original transformation to the CIELab from CIEXYZ is a non-linear one [13]. The nonlinearity in the transformation from CIELab distorts the spatially averaged tone of the images, which yields halftones that have incorrect average values [9]. The linearized color space overcomes this, and has the added benefit that it decouples the effect of incremental changes in (Y_y, C_x, C_z) at the white point on (L, a, b) values:

$$\nabla_{(Y_y, C_x, C_z)}(L^*, a^*, b^*)|_{D_{65}} = \frac{1}{3}\mathbf{I} \tag{4}$$

B. Human Visual Frequency Response

Nasanen and Sullivan [14] chose an exponential function to model the luminance frequency response

$$W_{(Y_y)}(\tilde{\rho}) = K(L)e^{-\alpha(L)\tilde{\rho}} \tag{5}$$

where L is the average luminance of display, $\tilde{\rho}$ is the radial spatial frequency, $K(L) = a\,L^b$ and $\alpha(L) = \frac{1}{c\ln(L)+d}$. The frequency variable $\tilde{\rho}$ is defined [9] as a weighted magnitude of the frequency vector $\mathbf{u} = (u, v)^T$, where the weighting depends on the angular spatial frequency ϕ [14]. Thus,

$$\tilde{\rho} = \frac{\rho}{s\,(\phi)},\ \textit{where}\ \rho = \sqrt{u^2 + v^2}\ \textit{and}\ s\,(\phi) = \frac{1-\omega}{2}\cos(4\phi) + \frac{1+\omega}{2} \tag{6}$$

The symmetry parameter ω is 0.7, and $\phi = \arctan\left(\frac{v}{u}\right)$. The weighting function $s\,(\phi)$ effectively reduces the contrast sensitivity to spatial frequency components at odd multiples of 45^o. The contrast sensitivity of the human viewer to spatial variations in chrominance falls off faster as a function of increasing spatial frequency than does the response to spatial variations in luminance [15]. Our chrominance model reflects this [16]:

$$W_{(C_x,C_z)}(\rho) = Ae^{-\alpha\rho} \tag{7}$$

Both the luminance and chrominance response are lowpass in nature but only the luminance response is reduced at odd multiples of 45^o. This will place more luminance error across the diagonals in the frequency domain where the eye is less sensitive. Using this chrominance response as opposed to identical reponses for both luminance and chrominance will allow more low frequency chromatic error, which will not be perceived by the human viewer.

IV. Tone Dependent Color Error Diffusion

A. Perceptual Error Metric

We train error filters to minimize a visually weighted squared error between the magnitude spectra of a "constant" input color image and its halftone pattern. Let $x_{(R,G,B)}(\mathbf{m})$ and $b_{(R,G,B)}(\mathbf{m})$ denote the constant valued continuous tone and halftone images respectively. Then, $x_{(Y_y,C_x,C_z)}(\mathbf{m})$ and $b_{(Y_y,C_x,C_z)}(\mathbf{m})$ are the obtained by transforming $x_{(R,G,B)}(\mathbf{m})$ and $b_{(R,G,B)}(\mathbf{m})$ to the $Y_yC_xC_z$ space. The calculation of the perceptual error metric is illustrated in Fig. 2. The constant valued continuous tone color image and its halftone pattern are transformed to the $Y_yC_xC_z$ space. The difference in their spectra $\mathbf{Err}(k,l)$ is computed as $\mathbf{Err}(k,l) = \mathbf{X}_{(Y_y,C_x,C_z)}(k,l) - \mathbf{B}_{(Y_y,C_x,C_z)}(k,l)$ where $\mathbf{X}_{(Y_y,C_x,C_z)}(k,l) = FFT(x_{(Y_y,C_x,C_z)}(\mathbf{m}))$ and $\mathbf{B}_{(Y_y,C_x,C_z)}(k,l) = FFT(b_{(Y_y,C_x,C_z)}(\mathbf{m}))$. Human visual filters as discussed in Section III, are applied to the luminance and chrominance components of the error image in the spatial frequency domain. This corresponds to a multiplication of the filter spectra and the error image spectra $\mathbf{P}(k,l) = \mathbf{Err}(k,l)\mathbf{H}_{HVS}(k,l)$. Here, $\mathbf{H}_{HVS}(k,l)$ denotes the FFT of the human visual spatial filter. Note that, $\mathbf{P}(k,l)$, $\mathbf{H}_{HVS}(k,l)$ and $\mathbf{Err}(k,l)$ are vector valued. In particular they are 3×1 vectors with $\mathbf{Err}(k,l) = (Err_{Y_y}(k,l), Err_{C_x}(k,l), Err_{C_z}(k,l))$,

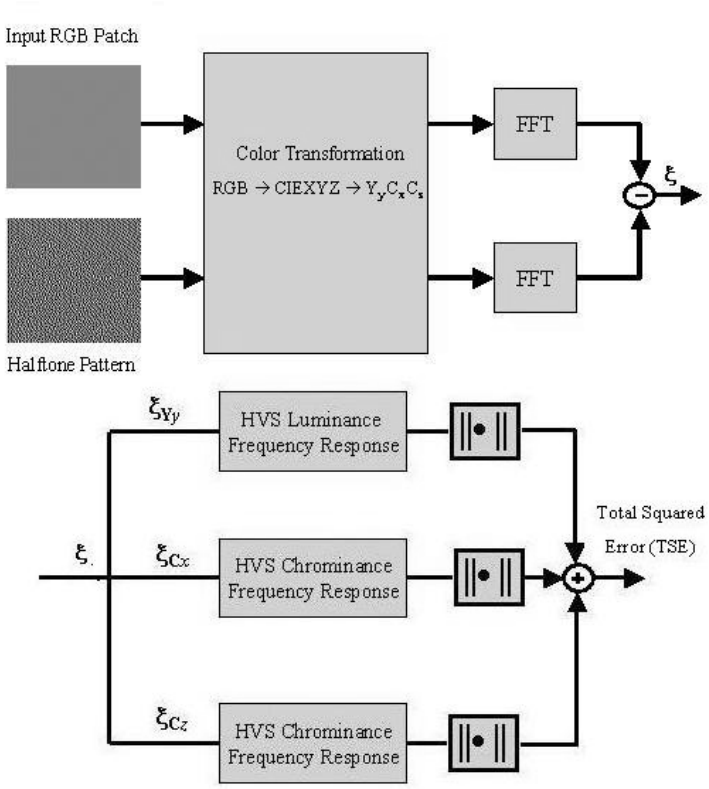

Fig. 2. Block Diagram for Calculating Perceptual Error Metric

$\mathbf{H}_{HVS}(k,l) = (H_{Lum}(k,l), H_{Chrom}(k,l), H_{Chrom}(k,l))$ and $\mathbf{P}(k,l) = (P_{Y_y}(k,l), P_{C_x}(k,l), P_{C_z}(k,l))$. We define the perceived error metric as the total squared error (TSE) given by

$$TSE = \sum_k \sum_l |P_{Y_y}(k,l)|^2 + |P_{C_x}(k,l)|^2 + |P_{C_z}(k,l)|^2 \tag{8}$$

B. Formulation of the Design Problem

The design problem is then to obtain error filters for each color plane that minimize the TSE defined in eqn. (8), subject to the constraints that all quantization error to be diffused

$$\sum_{\mathbf{k}\in\mathcal{S}} h_m(\mathbf{k};a) = 1, h_m(\mathbf{k};a) \geq 0 \quad \forall \quad \mathbf{k} \in \mathcal{S} \tag{9}$$

where the subscript m takes on values R, G and B and hence the constraints are imposed on error filters in each of the 3 color planes. The error filter coefficients are a function of the input tone a. The design objective is to obtain error filter weights for each (R,G,B) vector in the input. This would amount to a total of 256^3 input combinations. We consider input values along the diagonal line of the color cube i.e. $(R,G,B) = ((0,0,0),(1,1,1)....(255,255,255))$. This results in 256 error filters for each color plane. It should be realized that the TSE is in general not a convex function. Hence, a global minimum cannot be guaranteed.

(a) Original Color Ramp Image

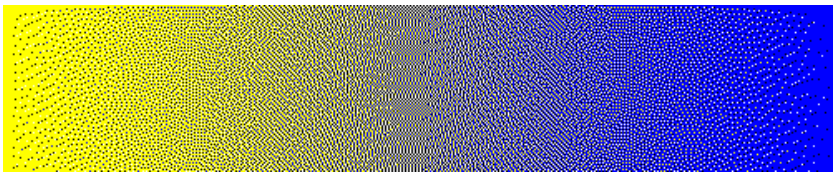

(b) Floyd-Steinberg error diffusion

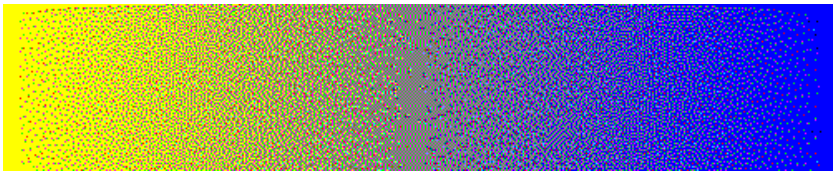

(c) Tone Dependent Error Diffusion (TDED) with serpentine scan

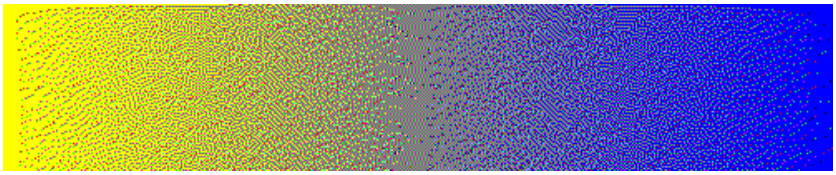

(d) Tone Dependent Error Diffusion (TDED) with traditional raster scan

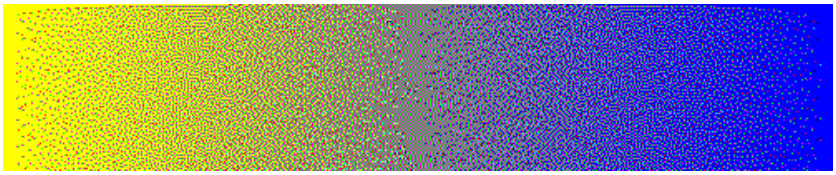

(e) Tone Dependent Error Diffusion (TDED) with 2-row serpentine scan

Fig. 3. Halftone images of color ramp generated by traditional and tone dependent error diffusion

The space of solutions (error filter weights) however comprises a convex set. The algorithm to search for the optimum error filter coefficients for each color plane is described in [7]. The design is based on a Floyd-Steinberg [1] support for the error filter.

V. Results

Fig. 3 shows halftone images generated by TDED with different scan paths. The traditional Floyd-Steinberg (FS) halftone Fig. 3(b) is also shown for comparison. The TDED halftone in Fig. 3(c) does not suffer from directional artifacts like diagonal worms. These can be seen in the FS halftone close to the yellow and blue

extremes of the ramp. False textures in the FS halftone are prominent in the middle of the yellow region (a third of the ramp length from the left) and in the centre of the ramp where yellow leads into blue. These are nearly absent in Fig. 3(c). The choice of color to render at extreme levels is also better for the TDED halftone. In Fig. 3(b) white dots are rendered close to the extreme blue regions of the ramp. These are replaced by a mixture of magenta, cyan and black dots in the TDED halftone which are less visible. Detail of the halftones in Fig. 3(b) and (c) are shown in Fig. 4(a) and (b). Diagonal worms are not present in the TDED halftone and the visibility of the halftone pattern is minimized as well. Serpentine scan generates the best results with TDED. The conventional raster scan (Fig. 3(d)) still shows the tendency for dots/holes to line up in horizontal or diagonal worms particularly at extreme levels. While the serpentine scan with TDED almost completely removes directional artifacts, it can only be executed as a serial process. A 2-row serpentine scan [7] employed in Fig. 3(e) generates results comparable to Fig. 3(c) and is more parallelizeable.

The results in Fig. 5 explain the role of color HVS model. Note that the green diagonal worms in the shadow region (extreme levels) under the roof that appear in the FS halftone (Fig. 5 (a)) are pretty much removed in Fig. 5(b). Monochrome images corresponding to the Y_y and C_x components of the FS and TDED halftones are presented in Fig. 5(c) through (f). The Y_y component is obtained by converting the final halftone to the $Y_yC_xC_z$ color space and setting both the C_x and C_z components to zero, resulting in $(Y_y, 0, 0)$. The resulting vector is transformed back to the RGB space for display. The C_x component is obtained similarly. Comparing Fig. 5(c) and (d) for FS error diffusion, we see that both the Y_y and C_x components exhibit similar texture. In contrast, we see in Fig. 5(e) and (f), the C_x component has much lower frequency texture than the Y_y component owing to the more agressive HVS filtering of the chrominance planes. When viewed as true color images the overall halftone texture is much less visible in the TDED halftone.

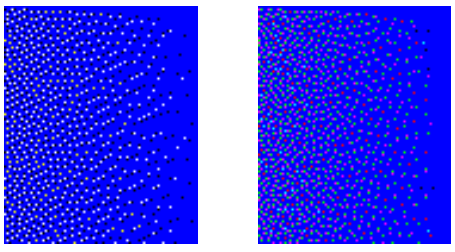

(a) Floyd-Steinberg (b) TDED

Fig. 4. Detail of the Floyd-Steinberg and TDED halftones, blue region (extreme right) of the color ramp

VI. Conclusion

An input level (tone) dependent color halftoning algorithm was proposed. A linear channel-separable color HVS model is used to design visually optimum error filters for each color plane. The resulting halftones are seen to overcome most traditional error diffusion halftoning artifacts. Future work may investigate the design of optimum matrix valued filters for tone dependent vector color error diffusion halftoning.

References

[1] R. Floyd and L. Steinberg, "An adaptive algorithm for spatial grayscale," *Proc. Soc. Image Display*, vol. 17, 1976.

[2] N. Damera-Venkata and B. L. Evans, "Adaptive threshold modulation for error diffusion halftoning," *IEEE Trans. on Image Processing*, vol. 10, no. 1, pp. 104–116, Jan. 2001.

[3] J. Sullivan, R. Miller, and G. Pios, "Image halftoning using a visual model in error diffusion," *J. Opt. Soc. Am. A*, vol. 10, no. 8, pp. 1714–1724, Aug. 1993.

[4] R. Eschbach, "Error-diffusion algorithm with homogenous response in highlight and shadow areas," *J. Electronic Imaging*, vol. 6, pp. 1844–1850, 1997.

[5] P. Wong, "Adaptive error diffusion and its application in multiresolution rendering," *IEEE Trans. on Image Processing*, vol. 5, no. 7, pp. 1184–1196, July 1996.

[6] R. Ulichney, *Digital Halftoning*, MIT Press, Cambridge, MA, 1987.

[7] P. Li and J. P. Allebach, "Tone dependent error diffusion," *SPIE Color Imaging: Device Independent Color, Color Hardcopy, and Applications VII*, vol. 4663, pp. 310–321, Jan. 2002.

[8] R. Eschbach, "Reduction of artifacts in error diffusion by means of input-dependent weights," *J. Electronic Imaging*, vol. 2, no. 4, pp. 352–358, Oct. 1993.

[9] T. J. Flohr, B. W. Kolpatzik, R. Balasubramanian, D. A. Carrara, C. A. Bouman, and J. P. Allebach, "Model based color image quantization," *Proc. SPIE Human Vision, Visual Proc. and Digital Display IV*, vol. 1913, pp. 270–281, 1993.

[10] V. Monga, W. S. Geisler, and B. L. Evans, "Linear, color separable, human visual system models for vector error diffusion halftoning," *IEEE Signal Processing Letters*, vol. 10, Apr. 2003.

[11] V. Ostromoukhov, "A simple and efficient error-diffusion algorithm," *Proc. Int. Conf. on Computer Graphics and Interative Tech.*, Aug. 2001.

[12] K.T. Mullen, "The contrast sensitivity of human color vision to red-green and blue-yellow chromatic gratings," *Journal of Physiology*, 1985.

[13] M. D. Fairchild, *Color Appearance Models*, Addison-Wesley, 1998.

[14] J. Sullivan, L. Ray, and R. Miller, "Design of minimum visual modulation halftone patterns," *IEEE Trans. on Systems, Man, and Cybernetics*, vol. 21, no. 1, pp. 33–38, Jan. 1991.

[15] D. H. Kelly, "Spatiotemporal variation of chromatic and achromatic contrast thresholds," *Journal Opt. Soc. Amer. A*, vol. 73, pp. 742–750, 1983.

[16] B. Kolpatzik and C. Bouman, "Optimized error diffusion for high quality image display," *Journal of Electronic Imaging*, vol. 1, pp. 277–292, Jan. 1992.

(a) Floyd-Steinberg Halftone

(b) TDED Halftone

(c) Y_y component of the FS halftone

(d) C_x component of the FS halftone

(e) Y_y component of the TDED halftone

(f) C_x component of the TDED halftone

Fig. 5. (a) Floyd-Steinberg and (b) TDED halftones of the house image